Optics and Laser Technology 100 (2018) 103–108

Contents lists available at ScienceDirect

Optics and Laser Technology

journal homepage: www.elsevier.com/locate/optlastec

Full length article

Compact self-Q-switched Tm:YLF laser at 1.91 μm

B. Zhang [a,1], L. Li [a,*,1], C.J. He [a], F.J. Tian [a], X.T. Yang [b,*], J.H. Cui [a], J.Z. Zhang [a], W.M. Sun [a]

[a] Key Laboratory of In-fiber Integrated Optics of Ministry of Education, Harbin Engineering University, Harbin 150001, China
[b] College of Power and Energy Engineering, Institute of Marine Engine Electronic Control Technology, Harbin Engineering University, Harbin 150001, China

ARTICLE INFO

Article history:
Received 19 June 2017
Received in revised form 2 September 2017
Accepted 3 October 2017
Available online 7 November 2017

Keywords:
Diode-pumped
Solid-state laser
Q-switching
2 μm spectral region

ABSTRACT

We report self-Q-switching operation in a diode-pumped Tm:YLF bulk laser by exploiting saturable re-absorption under the quasi-three-level regime. Robust self-Q-switched pulse output at 1.91 μm in fundamental mode is demonstrated experimentally with 1.5 at.% doped Tm:YLF crystal. At maximum absorbed pump power of 4.5 W, the average output power and pulse energy are obtained as high as 610 mW and 29 μJ, respectively, with the corresponding slope efficiency of 22%. Pulse repetition rate is tunable in the range of 3–21 kHz with changing the pump power. The dynamics of self-Q-switching of Tm:YLF laser are discussed with the help of a rate equation model showing good agreement with the experiment. The compact self-Q-switched laser near 2 μm has potential application in laser radar systems for accurate wind velocity measurements.

1. Introduction

Thulium (Tm) doped solid-state lasers operating in the 2-μm eye-safe spectral range are of interest for applications in photo-medicine, laser ranging and infrared lidar [1]. Q-switched 2-μm lasers are especially important for pumping optical parametric oscillators (OPO) for efficient conversion into the mid-infrared [2]. By using active or passive Q-switch elements, pulsed 2-μm laser sources have been widely obtained. Actively Q-switching operation can be obtained by introducing acousto-optical (AO) or electro-optical (EO) devices into laser cavity to provide optical shutters [3,4]. Passively Q-switching at 2 μm can be initiated by nonlinear saturable absorbers (SA), such as InGaAs/GaAs, Cr:ZnS and Cr:ZnSe crystals, graphene and carbon nanotube [5–7]. In comparison with the approaches of introducing AO/EO devices or SA elements, self-Q-switching as an available mechanism to generate pulse output is far simple and compact in laser architecture and low cost since no additional modulation components are needed [8].

Self-Q-switching was first performed in ruby lasers without additional Q-switch element [9]. Self-Q-switching operation at 1-μm spectral region has been widely achieved in Nd-doped, Cr, Nd-codoped, Yb-doped, and Cr,Yb-codoped lasers [10–14]. However, few studies has been reported on self-Q-switched solid-state lasers at 2-μm region. Razdobreev et al. demonstrated the self-Q-switching operation of monolithic Tm:YAP microlaser at 1.94 μm [15]. Stable self-pulsing output was obtained at high pump power beyond a certain threshold due to the phonon-assisted excited-state absorption (ESA) mechanism. Such self-pulsing regime is basically different from the relaxation oscillation instabilities observed in continuous wave (CW) Tm:YAP and Tm:YAG lasers [16]. Wu et al. presented a chaos analysis of self-pulsing output of Tm:YAP laser [17]. Nonlinear dynamical chaos regime was proposed to explain the self-Q-switching of Tm:YAP laser, but the physical parameters responsible for the chaotic behavior are unknown till now. Meanwhile, Cai et al. performed robust self-Q-switching operation in 5% doped Tm:YAP laser [18]. The time-dependent lens occurring inside the gain medium was believed responsible for self-Q-switching, which originates from refractive index changes induced by thermal lensing.

Compared with Tm:YAP, Tm:YLF crystal has been known as the excellent candidate to produce high power output at 2 μm region due to negative thermal lens, inherent linearly polarized output and high quantum yield [1,19]. With these favorable features, Tm:YLF lasers have been investigated by some workers with efforts to produce high power output towards the 100-W regime [19–23]. An optimized doping level of 2 at.% Tm:YLF with a slab geometry was shown experimentally to allow scaling of a single gain unit to output power of 70 and 148 W under single- and double-end-pumping schemes, respectively [21,22]. The actively and passively Q-switched Tm:YLF lasers has been studied to generate high energy pulses. With deploying the fused silica AO modulator as an active Q-switch, an end-pumped Tm:YLF laser was

* Corresponding authors.
E-mail addresses: lylee_heu@hrbeu.edu.cn (L. Li), yangxiaotao1985@163.com (X.T. Yang).
[1] These authors contributed equally to this work.

https://doi.org/10.1016/j.optlastec.2017.10.001
0030-3992/

demonstrated to be capable of outputting up to 10-mJ pulse energy at 133 Hz repetition rate [24]. By using polycrystalline Cr^{2+}:ZnSe as a SA, stable passively Q-switching of Tm:YLF laser was obtained with highest pulse energy of 4.2 mJ at repetition rate of below 450 Hz [7]. Additionally, tunable CW operation of 1.5% Tm:YLF laser at 2.3 μm region has been demonstrated with maximum output power of 200 mW, showing the continuous tunability in the spectra from 2.20 to 2.46 μm [25]. By using Cr^{2+}:ZnSe SA, passively Q-switched operation of 2.3 μm Tm:YLF laser has been obtained with maximum output power of 27 mW and pulse energy of 13 μJ under double-end-pumping [26]. However, stable self-Q-switching of Tm:YLF laser near 2 μm has not been reported yet.

In the paper, self-Q-switched operation in a diode-pumped Tm:YLF bulk laser at 1.91 μm is demonstrated experimentally. The saturable re-absorption effect of Tm:YLF laser with quasi-three-level nature is exploited to initiate self-Q-switching. At maximum absorbed pump power of 4.5 W, the average output power and pulse energy are achieved as high as 610 mW and 29 μJ, respectively, with the corresponding slope efficiency of 22% and repetition rate of 21 kHz. The self-Q-switching dynamics of Tm:YLF laser is discussed with the help of rate equation model showing good agreement with the experimental. It is of interest in understanding the origin of self-Q-switching of Tm-doped solid-state laser near 2 μm.

2. Experimental setup

Fig. 1 shows a schematic of the experimental setup used to obtain self-Q-switched operation of Tm:YLF laser. The pump source is a fiber-coupled diode laser with 10-W maximum CW power at 790 nm (spectral linewidth ~2 nm). The fiber core diameter is 400 μm, and the numerical aperture (NA) is 0.22. The pump beam is collimated and focused by a 1:1 coupling lens group into a pump spot radius of ~200 μm on the Tm:YLF crystal. In order to maximize the average output power, the pump spot on the crystal is optimized by slightly adjusting the focusing lens position during the experiment. The *a*-cut 1.5% Tm:YLF crystal with dimensions of $3 \times 3 \times 10\ mm^3$ was wrapped in Indium foil and mounted in a water-cooled copper holder for heat dissipation. The circulating water temperature maintained at 286 K. Both end faces of Tm:YLF crystal were anti-reflection coated for high transmission (T > 99.5%) in the spectra of 1.9–2.1 μm and at 790 nm pump wavelength. The pump absorption at 790 nm by the crystal is about 74%. A compact linear resonator is adopted, with 145-mm cavity length. The dichroic input plane mirror (M1) is high reflection coated at 1.9–2.1 μm and anti-reflection coated at 780–800 nm. The output coupler (M2) is a plano-concave mirror with 150 mm curvature radius that is partially reflective with a 98% reflection coefficient at 1.9 μm band. By using ABCD matrix, the laser mode distribution in the cavity was simulated. The laser mode radius in the crystal is around 130 μm. The pump-to-mode ratio of 1.5 leads to optimal overlap efficiency, which is desirable to restrain random relaxation oscillations and fractional thermal loading [27,28].

The laser output was measured by a Coherent FieldMaxII laser power meter and an InGaAs photodiode. The spectrum of the laser was monitored by a Zolix monochromator (Omni-λ 3015, resolution of the spectrum is 0.1 nm). The pulse trains were recorded by a 300 MHz bandwidth digital oscilloscope (Tektronix TDS3032B) with a > 100 MHz bandwidth IR detector (Vigo PVM-10.6).

3. Results and discussion

Fig. 2 shows the average output power of self-Q-switched Tm:YLF laser with respect to the absorbed pump power. The threshold of pump absorption power is 1 W. At maximum absorbed pump power of 4.5 W, up to 610 mW of average power was obtained with the corresponding slope efficiency of 22%. No saturation of laser output was observed in experiment, which means that the higher power output can be achieved if more pump power is available. Beyond the pump threshold, a train of self-Q-switched pulses with full depth of modulation can be observed but the repetition rate varies with the pump power. The inset of Fig. 2 shows a typical pulse train at 3 W of absorbed pump power with the repetition rate

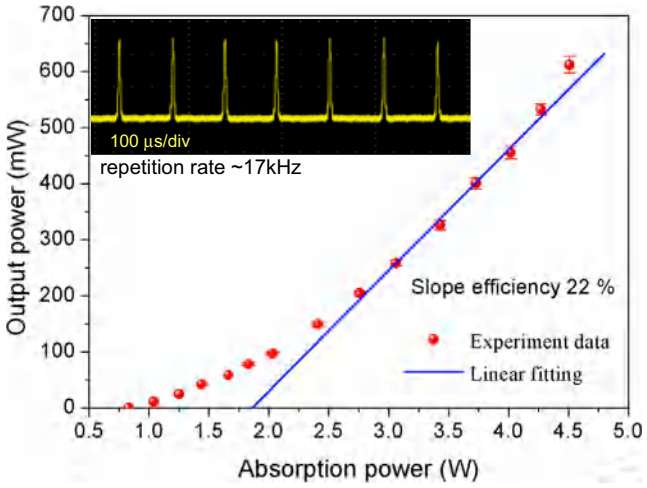

Fig. 2. Average output power in self-Q-switched operation of Tm:YLF laser. (Inset) Recorded pulse train at 3 W of pump absorption power.

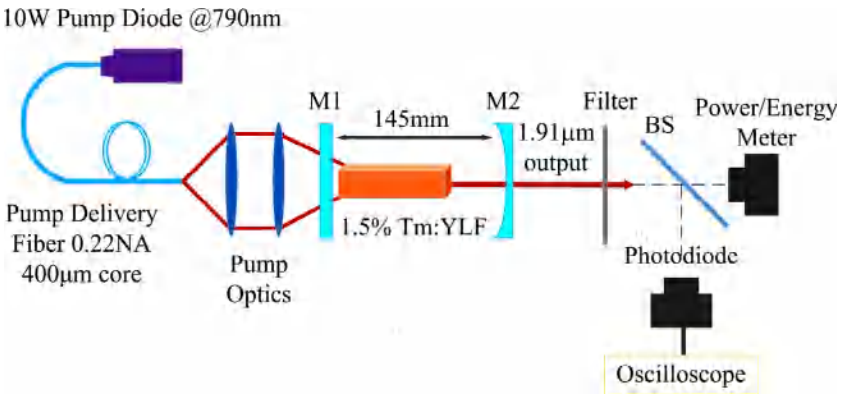

Fig. 1. Schematic experimental setup for self Q-switching operation in 1.5% Tm:YLF bulk laser at 1.91 μm.

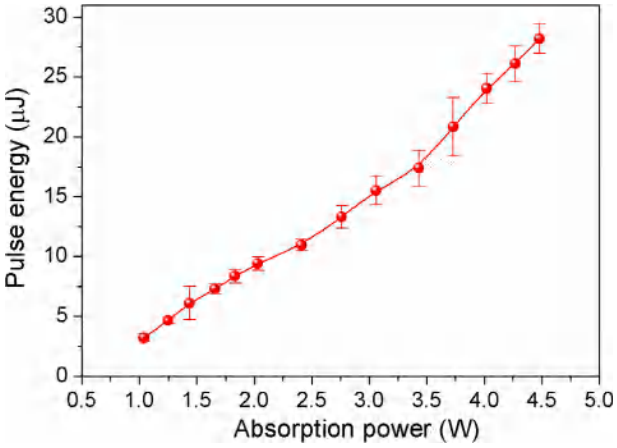

Fig. 3. Output pulse energy as the function of pump absorption power.

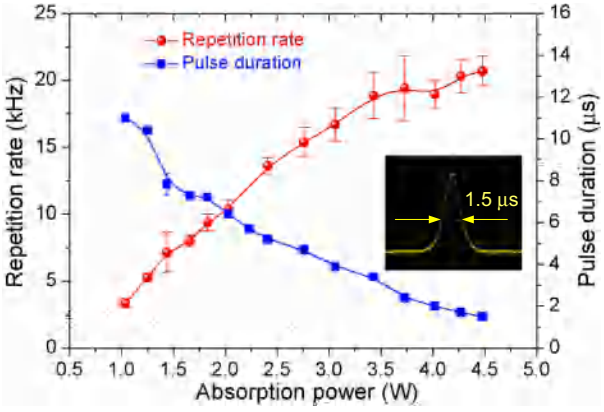

Fig. 4. The repetition rate and pulse duration as functions of absorbed pump power. (inset) Expended shape of the pulse at 4.5 W pumping.

of 17 kHz and highly symmetric pulse profiles. Robust pulsed laser oscillation can be improved by slightly tuning the alignment of pump beam and cavity mode [8]. The individual pulse energies at various pump powers were measured as shown in Fig. 3. The error analysis was indicated with different error bars to reflect the fluctuation of pulse energy and the error of measurement system. The pulse energy increases linearly with the pump power. At maximum absorbed pump power of 4.5 W, the large pulse energy of 29 μJ can be achieved.

The temporal characteristics of self-Q-switched pulse at various pump absorption powers were analyzed in experiment. Fig. 4 shows the repetition rate and pulse duration (full width at half maximum, FWHM) as functions of pump absorption power, respectively. As the pump absorption power increases from 1 to 4.5 W, the pulse repetition rate increases from 3 to 21 kHz. The pulse duration tends to be around 1.5 μs with temporal fluctuation less than 10%. The pulse fluctuation was mainly due to the mechanical and thermal perturbation. Fig. 4 also shows that the self-Q-switched pulse is highly symmetric in shape.

The spectral measurement of self-Q-switched Tm:YLF laser was carried out. As shown in Fig. 5, the lasing wavelength centers at 1.91 μm and multi-longitudinal modes may emerge since no effort was made to restrict the oscillating modes in the self-Q-switched operation. The output laser is linearly polarized along the *a*-axis of YLF crystal (σ polarized, $E \parallel a$-axis). The laser beam profile was characterized with a commercial beam analyzer, as shown in Fig. 5, which is close to the fundamental transverse electromagnetic mode (TEM_{00}).

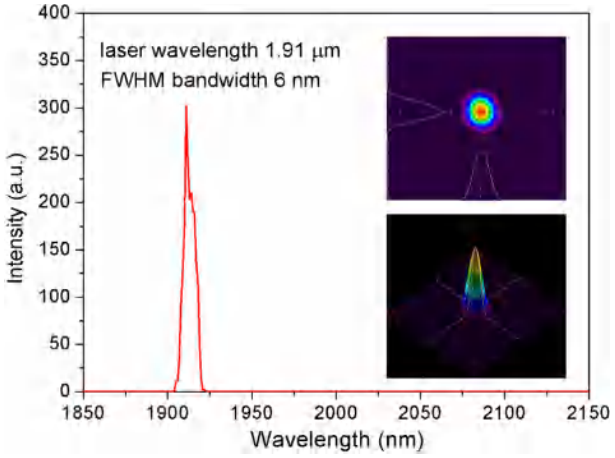

Fig. 5. Spectra and beam profile of pulse laser output. (inset) two dimensional pattern and three dimensional profile of laser beam.

It is worth mentioning that the thermal effect of Tm:YLF on self-Q-switched operation is negligible. In contrast to positive thermal lens of Tm:YAP, the negative lensing of Tm:YLF is partially compensated by the positive lens from surface bulging because Tm:YLF has a decrease in refractive index with temperature [21]. The overall thermal lensing effect is very weak, especially for the σ-polarized emission at 1.9 μm as discussed in [21,22]. Moreover during the experiment, the pump density is not strong, which is 4.5-W pump absorption power on a spot diameter of 400 μm. The fractional thermal loading is also restrained by optimal pump-to-mode ratio as suggested in [27,28]. This indicates that the self-Q-switching of Tm:YLF laser does not originate from the mechanism of time-dependent lens which occurs in Tm:YAP laser. Additionally, the optimal 1.5% Tm:YLF can remarkably suppress the phonon-assisted ESA of Tm^{3+} $^3H_5 \rightarrow {}^3H_4$ transition due to the smaller phonon energy than those of oxide hosts (phonon energy of YLF ~560 cm^{-1}) [25,29–32]. It is suggested that the self-Q-switching of Tm:YLF laser is not closely associated with the ESA mechanism. However, in Tm:YLF lasers, the quasi-three-level regime of laser transition can result in thermal population at the lower laser level (a Stark splitting level at $^3H_6$), which leads to GSRA effect [29]. The GSRA loss is saturable in nature, so it can provide an available mechanism of self-Q-switching. Meanwhile, large modulation depth of self-pulsed output can be expected due to the larger cross section of GSRA in Tm:YLF than that of ESA in Tm:YAP. Note that the analysis of self-Q-switching from the view of saturable re-absorption was previously presented in Nd:YVO_4 laser at 914 nm and Yb:KGdW near 1044 nm and Er:Lu_2O_3 at 2.7 μm [8,10–14,33].

Based on the consideration above, the self-Q-switched operation of Tm:YLF laser can be attributed to the saturable GSRA mechanism resulting from thermal population at $^3H_6$ state. Fig. 6 shows the level schematic of Tm ion mainly involving pump-to-laser energy transport and GSRA processes. The precisely-calibrated Stark splitting levels (fine spectra) information of Tm^{3+} in YLF crystal were summarized in Ref. [34] (Table XII therein). Taking into account quasi-three-level laser character, the rate equations of a CW-pumped Tm:YLF laser can be written as [33,35,36]

$$\frac{dn(t)}{dt} = f_{12}\frac{\eta_c\eta_a P_{in}}{\pi\omega_p^2 lh\nu_p} - f_{12}\frac{\sigma\phi(t)}{\pi\omega_l^2 T_c}n(t) - \frac{n(t)+f_1 N}{\tau_f} \quad (1)$$

$$\frac{d\phi(t)}{dt} = \frac{\phi(t)}{T_c}[2l\sigma n(t) - L_0 - \log(1/R) - Q(t)] + \pi\omega_p^2 l\frac{n(t)}{\tau_f} \quad (2)$$

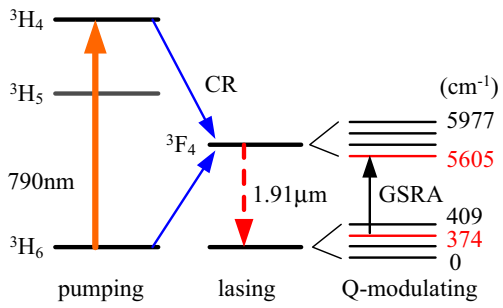

Fig. 6. Schematic of Tm^{3+} energy level diagram presenting the pump-to-laser energy transport involved in self-Q-switching mechanism. CR represents the cross relaxation process. GSRA indicates the ground-state re-absorption process. The Stark splitting levels matching with the lasing transition are marked with energies (cm^{-1}) according to [34].

$$Q(t) = \sigma f_1 N l \frac{I_s}{I(t)} \ln\left(1 + 2\frac{I(t)}{I_s}\right) \tag{3}$$

$$I_s = \frac{h\nu}{f_{12}\sigma\tau_f}, \quad I(t) = \phi(t)\frac{h\nu}{\pi\omega_l^2 T_c}, \tag{4}$$

In the equations, $n(t)$ and $\phi(t)$ denote the instantaneous population inversion density and intracavity photon number, respectively. P_{in} is incident pump power and η_a is the absorption efficiency. ν_p is the pump photon frequency and ω_p is the pump spot radius. h is Planck's constant. η_c denotes the quantum yield of cross relaxation, which is usually between one and two [21]. σ indicates the cross section of stimulated emission. ω_l and T_c are the radius and lifetime of cavity mode. τ_f is the lifetime of metastable $^3F_4$ state. $f_{12} = f_1 + f_2$, where f_1 (f_2) represents the fractional population at the lower (upper) laser level. l denotes the length of Tm:YLF crystal. L_0 is the intrinsic cavity loss. R is the reflectivity of output mirror. N is the total concentration.

In the model, Eq. (1) represents the rate of change of the population inversion between $^3F_4$ and $^3H_6$ laser levels. Eq. (2) governs the rate of build-up of cavity mode photon density. Eq. (3) characterizes the GSRA process leading to self-Q-switching of Tm:YLF laser. Eq. (4) describes the saturable intensity and the instantaneous intensity associated with GSRA process [33,35]. The physical model includes all dominant processes shown in Fig. 6. On the basis of experimental measurement, the parameters used for numerical simulations are summarized. $l = 10$ mm, $R = 0.98$, $\eta_a = 0.74$, $\omega_p = 200$ μm, $\tau_f = 15$ ms, $\sigma = 3 \times 10^{-21}$ cm^2, $\eta_c = 1.6$, $L_0 = 0.01$, $T_c = 5$ ns, $\omega_l = 130$ μm and $N = 2.1 \times 10^{20}$ cm^{-3} for a Tm doping of 1.5% in YLF crystal [29,30,37–40]. $\nu_p = c/\lambda_p$ and $\nu = c/\lambda_l$ with $\lambda_p = 790$ nm, $\lambda_l = 1.91$ μm, and $c = 3 \times 10^8$ m/s. The values of f_1 and f_2 can be estimated by Boltzmann distribution law on the basis of available Stark splitting levels information given in [34], and were found to be $f_1 = 0.04$ and $f_2 = 0.37$ at the operation temperature, respectively. The set of rate equations are solved numerically by the fourth-order Runge–Kutta method to simulate the dynamics of self-Q-switched operation in Tm:YLF laser.

Fig. 7 shows the theoretical reproduction of pulse sequence in the self-Q-switched operation, which corresponds to the experimental observation at 3 W of pump absorption power. As shown in Fig. 7(a), the simulated pulses are highly symmetric in pulse profile. The repetition rate of pulse sequence is about 17 kHz which is in good agreement with the measurement shown in Fig. 2.

Accompanied with pulse generation, the dynamics of GSRA loss and population inversion were simulated for deep insight into the self-Q-switching. As seen from Fig. 7(b) and (c), the GSRA loss exhibits periodic modulation. At the same time, the synchronous switching of population inversion takes place. The initial GSRA loss

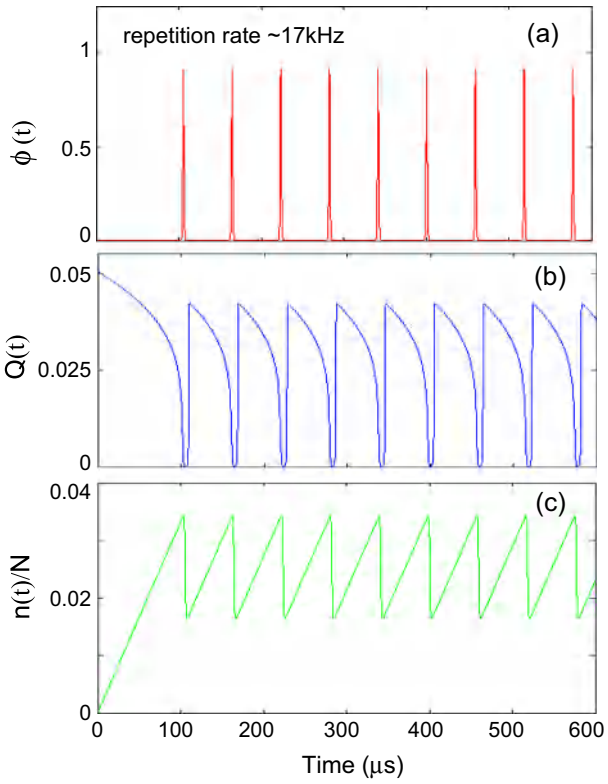

Fig. 7. Theoretical reproduction of pulse formation based on the rate equation model. (a) Pulse output at 1.91 μm with 17 kHz of repetition rate, (b) self Q-switching modulation, and (c) Population inversion dynamics normalized by total concentration.

value of ~0.05 is sufficiently high to hold-off the initial gain and no output occurs. As the CW pumping continues, the GSRA process becomes saturable and the re-absorption loss is suddenly reduced to zero. Consequently, a self-Q-switched pulse is generated. After emitting the first pulse, GSRA regains its initial loss value to hold-off the gain for storing next pulse energy. Such process continues to generate pulse sequence as shown in Fig. 7(a).

The simulation of repetition rate and pulse duration are plotted in Fig. 8. It shows that as the pump power (P_{in}/P_{th}) varies from 1 to 4.5, the repetition rate can increase from 6 to 24 kHz which are close to the experimental results (from 3 to 21 kHz in Fig. 4). The simulated pulse duration decreases with the pump power,

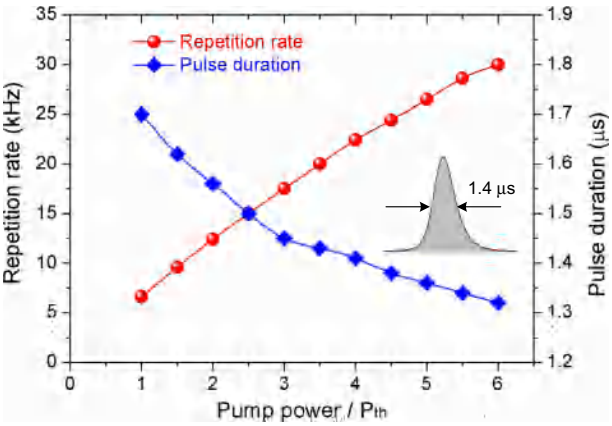

Fig. 8. Numerical simulation results for the repetition rate and pulse duration based on the rate equation model. (inset) Expended view of the pulse shape at $P_{in}/P_{th} = 4.5$ with highly symmetric profile.

noticeably at the threshold region, then tends to be around 1.4 μs at the pump power of P_{in}/P_{th} = 4.5. The pulse duration of 1.4 μs is close to the observed value of 1.5 μs shown by the inset of Fig. 4. Note that the experimental pulse durations are overall larger than the simulated ones. This is due to multi-longitudinal modes oscillation in self-Q-switched laser operation, which can considerably increase the pulse duration [33]. The assumption of single longitudinal mode in the model is responsible for the deviation of pulse width between the simulation and experimental results, because no effort was made to restrict the cavity modes in self-Q-switched laser setup. Additionally, the expended view of typical pulse is shown by the inset of Fig. 8. It is evident that the simulated pulse profile is highly symmetric in shape as observed experimentally.

In simulation, self-Q-switching was found to be strongly dependent on the fractional population (f_1) of Stark level at $^3H_6$ ground-state. The self-Q-switching can readily operate under the population fraction of $f_1 > 0.01$. Otherwise it will lead to the disappearance of self-Q-switching and restoring of CW operation. The result indicates that the self-Q-switching of Tm:YLF laser is directly associated with the ground-state re-absorption. Regarding the origin of self-Q-switching in Tm-doped bulk laser, previously a four-level rate equation analysis suggested that the self-pulsing of monolithic Tm:YAP laser could be due to the ESA of $^3H_5 \rightarrow {}^3H_4$ transition [15]. However, the measurement of cross section for the ESA pointed out that it was too small to account solely for the self-pulsing. Nonlinear dynamical chaos as an alternative explanation was proposed based on experimental evidence of chaos in Tm:YAP laser [17]. Unfortunately, the physical parameters responsible for the chaotic behavior are still unknown. Meanwhile, the time-dependent lens effect occurring inside Tm:YAP crystal has been discussed to be the cause of self-Q-switching [19]. In contrast to the previous reports, our study presents a different, simple mechanism of self-Q-switching of Tm:YLF lasers, by exploiting saturable GSRA effect. It would be of interest in understanding the origin of self-Q-switching of Tm-doped bulk laser and providing available scheme for self-pulsing output.

4. Conclusion

In conclusion, self Q-switched operation in a diode-pumped Tm:YLF laser has been demonstrated by exploiting saturable GSRA effect under the quasi-three-level regime. Self-Q-switched pulse output with full depth of modulation has been obtained in the fundamental mode operation. Pulse repetition rate is tunable in the range of 3–21 kHz with changing the pump power. At maximum absorbed pump power of 4.5 W, the average output power and pulse energy at 1.91 μm has been achieved as high as 610 mW and 29 μJ, respectively, with the corresponding slope efficiency of 22%. The dynamics of self-Q-switched operation has been explained with the help of rate equation model. The simulation results show good agreement with the experimental. The study is of interest in understanding the origin of self-pulsing of Tm-doped solid-state lasers. The compact Tm:YLF pulse laser near 2 μm has potential application in lidar systems for accurate wind velocity measurements.

Acknowledgments

The authors acknowledge funding from National Natural Science Foundation of China (10804022), Natural Science Foundation of Heilongjiang (A201405), Postdoctoral Scientific research development fund of Heilongjiang (LBH-Q16061), 111 project to Harbin Engineering University (B13015), Fundamental Research Funds for the Central Universities.

References

[1] U.N. Singh, B.M. Walsh, J. Yu, M. Petros, M.J. Kavaya, T.F. Refaat, N.P. Barnes, Twenty years of Tm:Ho:YLF and LuLiF laser development for global wind and carbon dioxide active remote sensing, Opt. Mater. Express 5 (2015) 827.
[2] A. Godard, Infrared (2–12 μm) solid-state laser sources: a review, C. R. Physique. 8 (2007) 1100–1128.
[3] J. Zhao, Y. Li, S. Zhang, L. Li, X. Zhang, Diode-pumped actively Q-switched Tm:YAP/$BaWO_4$ intracavity Raman laser, Opt. Express 23 (2016) 10075–10080.
[4] P. Meng, B. Yao, G. Li, Y. Ju, Y. Wang, Comparison of RTP electro-optic Q-switch and acousto-optic Q-switch in Tm, Ho:$GDVO_4$ laser, Laser Phys. 21 (2011) 348–351.
[5] D. Sebbag, A. Korenfeld, U. Ben-Ami, D. Elooz, E. Shalom, S. Noach, Diode end-pumped passively Q-switched Tm:YAP laser with 1.85-mJ pulse energy, Opt. Lett. 40 (2015) 1250–1253.
[6] B. Yao, Y. Tian, G. Li, Y. Wang, InGaAs/GaAs saturable absorber for diode-pumped passively Q-switched dual-wavelength Tm:YAP lasers, Opt. Express 18 (2010) 13574–13579.
[7] A. Korenfeld, D. Sebbag, U. Ben-Ami, E. Shalom, G. Marcus, S. Noach, High pulse energy passively Q-switching of a diode-pumped Tm:YLF laser by Cr:ZnSe, Laser Phys. Lett. 12 (2015) 045804.
[8] L. Wang, H. Huang, D. Shen, J. Zhang, H. Chen, D. Tang, Highly stable self-pulsed operation of an Er:Lu_2O_3 ceramic laser at 2.7 μm, Laser Phys. Lett. 14 (2017) 045803.
[9] I. Freund, Self-Q-switching in ruby lasers, Appl. Phys. Lett. 12 (1968) 388–390.
[10] J. Dong, P. Deng, Y. Lu, Y. Zhang, Y. Liu, J. Xu, W. Chen, Laser-diode-pumped Cr^{4+}, N^{d3}+:YAG with self-Q-switched laser output of 1.4 W, Opt. Lett. 25 (2000) 1101–1103.
[11] S. Li, S. Zhou, P. Wang, Y.C. Chen, K.K. Lee, Self-Q-switched diode-end-pumped Cr, Nd:YAG laser with polarized output, Opt. Lett. 18 (1993) 203–205.
[12] M. Jiang, Q. Zhang, K. Qiu, D. Zhang, B. Feng, Self-Q-switched Cr, Nd:YAG laser under direct 885 nm diode laser pumping, Opt. Commun. 285 (2012) 3684–3687.
[13] J. Dong, A. Shirakawa, S. Huang, Y. Feng, K. Takaichi, M. Musha, K.I. Ueda, A.A. Kaminskii, Stable laser-diode pumped microchip sub-nanosecond Cr, Yb:YAG self-Q-switched laser, Laser Phys. Lett. 2 (2010) 387–391.
[14] J. Liu, J. Tian, Z. Dou, M. Hu, Y. Song, Self-Q-switching in bulk Yb:$KGd(WO_4)_2$ laser, Chin. Opt. Lett. 13 (2015) 061407.
[15] I. Razdobreev, A. Shestakov, Self-pulsing of a monolithic Tm-doped $YAlO_3$ microlaser, Phys. Rev. A 73 (2006) 053815.
[16] J.F. Pinto, L. Esterovitz, Suppression of spiking behavior in flashpumped 2-μm lasers, IEEE J. Quantum. Electron. 30 (1994) 167–169.
[17] K.S. Wu, O. Henderson-Sapir, P.J. Veitch, M. Hamilton, J. Munch, D.J. Ottaway, Self-pulsing in Tm-doped $YAlO_3$ lasers: excited-state absorption and chaos, Phys. Rev. A 91 (2015) 043819.
[18] W. Cai, J. Liu, C. Li, H. Zhu, P. Ge, L. Zheng, L. Su, J. Xu, Compact self-Q-switched laser near 2 μm, Opt. Commun. 334 (2015) 287–289.
[19] Y. Shen, B. Yao, C. Qian, X. Duan, T. Dai, Y. Wang, 108-W diode-end-pumped slab Tm:YLF laser with high beam quality, Appl. Phys. B 118 (2015) 555–559.
[20] M. Schellhorn, High-power diode-pumped Tm:YLF laser, Appl. Phys. B 91 (2008) 71–74.
[21] S. So, J.I. Mackenzie, D.P. Shepherd, W.A. Clarkson, J.G. Betterton, E.K. Gorton, A power-scaling strategy for longitudinally diode-pumped Tm:YLF lasers, Appl. Phys. B 84 (2006) 389–393.
[22] M. Schellhorn, S. Ngcobo, C. Bollig, High-power diode-pumped Tm:YLF slab laser, Appl. Phys. B 94 (2009) 195–198.
[23] T. Wang, Y. Ju, X. Duan, B. Yao, X. Yang, Y. Wang, Narrow linewidth continuous wave diode-pumped Tm:YLF laser with a volume bragg grating, Laser Phys. Lett. 6 (2009) 117–120.
[24] J.K. Jabczynski, L. Gorajek, W. Zendzian, J. Kwiatkowski, H. Jelinkova, J. Sulc, M. Nemec, High repetition rate, high peak power, diode pumped Tm:YLF laser, Laser Phys. Lett. 6 (2009) 109–112.
[25] J.F. Pinto, L. Esterowitz, G.H. Rosenblatt, Tm^{3+}:YLF laser continuously tunable between 2.20 and 2.46 μm, Opt. Lett. 19 (1994) 883–885.
[26] F. Canbaz, I. Yorulmaz, A. Sennaroglu, 2.3-μm Tm^{3+}:YLF laser passively Q-switched with a Cr^{2+}:ZnSe saturable absorber, Opt. Lett. 42 (2017) 1656–1659.
[27] G.L. Zhu, A 60 W Tm:YLF laser with triple Tm:YLF rods, Chin. Phys. Lett. 32 (2015) 094207.
[28] Y.F. Chen, Pump-to-mode size ratio dependence of thermal loading in diode-end-pumped solid-state lasers, J. Opt. Soc. Am. B. 17 (2000) 1835–1840.
[29] B.M. Walsh, N.P. Barnes, M. Petros, J. Yu, U.N. Singh, Spectroscopy and modeling of solid state lanthanide lasers: application to trivalent Tm^{3+} and Ho^{3+} in $YLiF_4$ and $LuLiF_4$, J. Appl. Phys. 95 (2004) 3255–3271.
[30] D.F.D. Sousa, V. Peters, G. Huber, A. Toncelli, D. Parisi, M. Tonelli, Pump modulation frequency resolved excited state absorption spectra in Tm^{3+} doped YLF, Appl. Phys. B. 77 (2003) 817–822.
[31] M.P. Hehlen, A. Kuditcher, A.L. Lenef, H. Ni, Q. Shu, S.C. Rand, J. Rai, S. Rai, Nonradiative dynamics of avalanche upconversion in Tm:$LiYF_4$, Phys. Rev. B. 61 (2000) 1116–1128.
[32] I.F. Elder, M.J.P. Payne, Lasing in diode-pumped Tm:YAP, Tm, Ho:YAP and Tm, Ho:YLF, Opt. Commun. 145 (1998) 329–339.
[33] P.K. Gupta, A. Singh, S.K. Sharma, P.K. Mukhopadhyay, K.S. Bindra, S.M. Oak, Note: Self Q-switched Nd:YVO_4 laser at 914 nm, Rev. Sci. Instrum. 83 (2012) 046110.

[34] H.P. Jenssen, A. Linz, R.P. Leavitt, C.A. Morrison, D.E. Wortman, Analysis of the optical spectrum of Tm^{3+} in $LiYF_4$, Phys. Rev. B 11 (1975) 92–101.
[35] T.Y. Fan, R.L. Byer, Modeling and CW operation of a quasi-three-level 946 nm Nd:YAG laser, IEEE J. Quantum. Electron. 23 (1987) 605–612.
[36] Q. Li, B. Feng, Z. Zhang, T. Zhang, Direct numerical simulation of quasi-three-level passive Q-switched laser, Opt. Commun. 284 (2011) 3391–3398.
[37] B.M. Walsh, N.P. Barnes, B.D. Bartolo, Branching ratios, cross sections, and radiative lifetimes of rare earth ions in solids: Application to Tm^{3+} and Ho^{3+} ions in $LiYF_4$, J. Appl. Phys. 83 (1998) 2772–2787.
[38] S.A. Payne, L.L. Chase, L.K. Smith, W.L. Kway, W.F. Krupke, Infrared cross-section measurements for crystals doped with Er^{3+}, Tm^{3+}, and Ho^{3+}, IEEE J. Quantum. Electron. 28 (1992) 2619–2630.
[39] R. Faoro, M. Kadankov, D. Parisi, S. Veronesi, M. Tonelli, V. Petrov, U. Griebner, M. Segura, X. Mateos, Passively Q-switched Tm:YLF laser, Opt. Lett. 37 (2012) 1517–1519.
[40] P. Loiko, J.M. Serres, X. Mateos, S. Tacchini, M. Tonelli, S. Veronesi, D. Parisi, A.D. Lieto, K. Yumashev, U. Griebner, V. Petrov, Comparative spectroscopic and thermo-optic study of Tm:$LiLnF_4$ (Ln = Y, Gd, and Lu) crystals for highly-efficient microchip lasers at ~2 μm, Opt. Mater. Express 7 (2017) 844–854.